



Extreme rainfall and wind speed projections for Vanuatu

EXPLAINER



This publication should be cited as:

CSIRO, Federation University, Climate Comms (2023).
Extreme rainfall and wind speed projections for Vanuatu.
A report to the Van-KIRAP project. Commonwealth
Scientific and Industrial Research Organisation
(CSIRO) Technical Report, Melbourne, Australia.

The authors and contributors to the report:

Krishneel Sharma (Federation University)

Savin Chand (Federation University)

Soubhik Biswas (Federation University)

Leanne Webb (CSIRO)

Hamish Ramsay (CSIRO)

Geoff Gooley (CSIRO)

Kevin Hennessy (Climate Comms)

© Commonwealth Scientific and Industrial Research
Organisation (CSIRO) 2023. To the extent permitted by law, all
rights are reserved, and no part of this publication covered
by copyright may be reproduced or copied in any form or by
any means except with the written permission of CSIRO.

Important Disclaimer

CSIRO advises that the information contained in this publication
comprises general statements based on scientific research. The
reader is advised and needs to be aware that such information
may be incomplete or unable to be used in any specific
situation. No reliance or actions must therefore be made on that
information without seeking prior expert professional, scientific
and technical advice. To the extent permitted by law, CSIRO
(including its employees and consultants) excludes all liability to
any person for any consequences, including but not limited to all
losses, damages, costs, expenses and any other compensation,
arising directly or indirectly from using this publication (in part
or in whole) and any information or material contained in it.

CSIRO is committed to providing web accessible content
wherever possible. If you are having difficulties with
accessing this document please contact csiro.au/contact

The project team would like to acknowledge
Ellian Bangtor, Gina Ishmael, Raviky Talae
and Geoff Gooley for images used on the front cover.

Contents

| | |
|--|-----------|
| Summary | 1 |
| Introduction | 2 |
| 1. Rainfall and wind speed data and calibrations | 2 |
| 2. Tropical cyclone wind speed | 9 |
| Discussion | 15 |
| Conclusions | 15 |
| References | 16 |
| Appendices | 17 |
| Appendix A: Summary of projected changes in extreme rainfall across provinces under a high emissions pathway | 17 |
| Appendix B: Summary of projected changes in cyclone wind speed intensity across provinces under a high emissions pathway | 18 |

Summary

This report provides a brief overview of the dataset and methodology used to create projection information for extreme rainfall and extreme wind speed for various locations in Vanuatu. Results for two locations (Port Vila and Luganville) are shown as examples, while results for six provinces are presented in the Appendix. Two future time periods are considered (2040–2070 and 2070–2100), relative to a baseline of 1970–2000, for medium and high greenhouse gas emissions pathways (RCP4.5 and RCP8.5, respectively) using climate models from phase 5 of the Coupled Model Intercomparison Project (CMIP5).

For extreme daily rainfall with return periods of 10–100 years, the multi-model mean results for Port Vila showed an increase of about 21 % for 2040–2070 RCP4.5, 30 % for 2070–2100 RCP4.5, 40 % for 2040–2070 RCP8.5 and 70 % for 2070–2100 RCP8.5. The equivalent results for Luganville showed an increase of about 18 % for 2040–2070 RCP4.5, 27 % for 2070–2100 RCP4.5, 26 % for 2040–2070 RCP8.5 and 57 % for 2070–2100 RCP8.5. These increases have significant implications for future flood risk management strategies.

For tropical cyclone extreme daily wind speed with return periods of 10–100 years, the multi-model mean results showed an increase in intensity of about 3 % for Port Vila and Luganville by 2070–2100 for RCP8.5 (data were not available for 2040–2070 or RCP4.5). These small increases may have implications for future cyclone risk management strategies.



Introduction

Vanuatu is highly exposed to climate variability and change. The Green Climate Fund is supporting the Van-KIRAP Project which is delivering climate information services (CIS) to inform decision-making by sectors and communities in Vanuatu. This project is led by SPREP (Secretariat of the Pacific Regional Environmental Program) in partnership with VMGD (Vanuatu Meteorology & Geo-hazards Department) and delivery partners, including Australia's CSIRO (Commonwealth Scientific and Industrial Research Organisation) and Federation University, along with the APEC (Asia-Pacific Economic Co-operation) Climate Centre.

More specifically, Van-KIRAP demonstrates the application of CIS in five priority sectors: infrastructure, water, agriculture, fisheries and tourism. Sectoral case studies include climate change impact assessments for each of the sectors to facilitate the development and demonstration of the application of CIS at multi-decadal timescales.

Van-KIRAP builds the technical capacity of key sectoral stakeholders to use CIS, including climate data, information, tools and other science-based resources. The project supports enhanced coordination and dissemination of CIS products and services to inform climate change impact/risk assessments and associated adaptation planning at the sectoral level.

The water and infrastructure sectors require information about current and future extreme rainfall and wind. This technical report describes data and methods used to estimate extreme rainfall and wind speed intensity and frequency for Vanuatu. It is anticipated that the approach described in this report can be adopted for other countries in the Pacific, and elsewhere around the globe.

1. Rainfall and wind speed data and calibrations

Daily rainfall data

For historical and future daily rainfall, this report uses weather station data, ERA5 reanalysis data, and climate model data from Coupled Climate Model Intercomparison Project phase 5 (CMIP5) (Taylor et al., 2012).

Historical greenhouse gas emissions, medium future emissions (RCP4.5) and high future emissions (RCP8.5) pathways (Moss et al., 2010) were used in simulations undertaken by the seven CMIP5 models in the study (Table 1). These models were selected because (a) they perform well in simulating the current climate and (b) they represent a broad range of future climates.

Table 1. List of CMIP5 climate models used for rainfall analysis

| CMIP5 Models | Historical period | RCP8.5 period | RCP4.5 period |
|---------------------|-------------------|---------------|---------------|
| ACCESS1.0 | 1850–2005 | 2006–2100 | 2006–2100 |
| CanESM2 | 1850–2005 | 2006–2100 | 2006–2100 |
| GFDL-ESM2M | 1850–2005 | 2006–2100 | 2006–2100 |
| GISS-E2-H | 1850–2005 | 2006–2100 | 2006–2100 |
| IPSL-CM5A-LR | 1850–2005 | 2006–2100 | 2006–2300 |
| IPSL-CM5A-MR | 1850–2005 | 2006–2100 | 2006–2100 |
| NorESM1-M | 1850–2005 | 2006–2100 | 2006–2300 |

Since the above CMIP5 models have coarse spatial resolution (about 200 km between data points) and contain systematic biases, the data needed to be calibrated. This can be done using geospatial interpolation (Li and Heap, 2014) and bias correction (Piani et al., 2010). The following three steps were carried out to calibrate the CMIP5 model data.

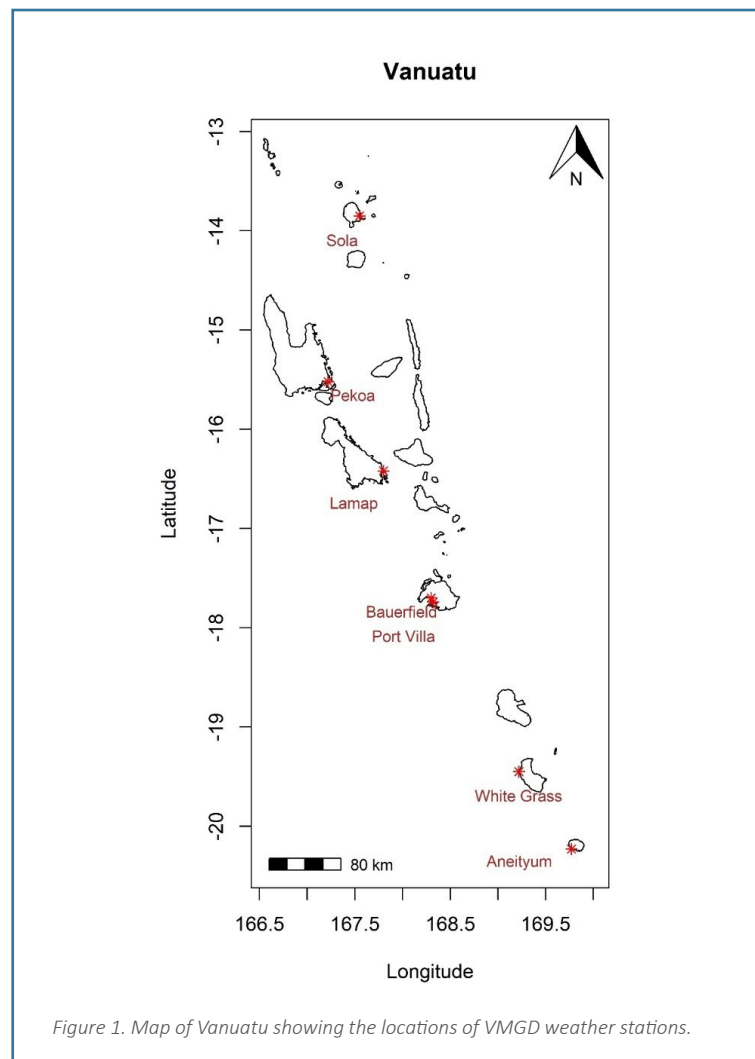
1. Fill in missing values in weather station data.
2. Calibrate ERA5 reanalysis data on a 30 km grid using weather station data.
3. Interpolate and bias-correct the climate model data using the calibrated ERA5 data.

Step 1

Temporal homogeneity was ensured for daily rainfall data obtained from seven VMGD weather stations (see Table 2 and Figure 1) across Vanuatu by filling in missing values using the inverse distance weighting (IDW) interpolation technique. IDW was chosen for its simplicity and low computational expense (Li and Heap, 2014).

Table 2. List of VMGD weather stations

| Station Name | Latitude (°E) | Longitude (°S) |
|--------------|---------------|----------------|
| Sola | 167.55 | 13.85 |
| Pekoa | 167.22 | 15.52 |
| Lamap | 167.8 | 16.42 |
| Bauerfield | 168.3 | 17.7 |
| Port Vila | 168.32 | 17.74 |
| White Grass | 169.22 | 19.45 |
| Aneityum | 169.77 | 20.23 |



Step 2

The ERA5 reanalysis dataset is available on a 30 km grid from 1940–2022. The daily accumulated rainfall for ERA5 is calculated from hourly ERA5 rainfall after accounting for the local time zone conversion from UTC. The ERA5 daily accumulated rainfall data were then calibrated with the VMGD weather station data nearest to each grid point. This was done using quantile-quantile matching (bin size of 450) with the help of a cubic spline approach; this approach does not assume linearity and is more appropriate for calibration of extremes (Biswas et al., 2022). The 1961–2005 data were used as the training period to calibrate the ERA5 daily accumulated rainfall from weather station daily rainfall data (Table 3).

Table 3. ERA5 and station data for rainfall

| Data | Station data | ERA5 | Calibrated ERA5 |
|----------------------------|--------------|---------------|-----------------|
| Spatial resolution | NA | 0.25° X 0.25° | 0.25° X 0.25° |
| Temporal resolution | Daily | Hourly | Daily |
| Time period | 1961–2022 | 1960–2022 | 1961–2005 |

Step 3

The CMIP5 model data were then bilinearly interpolated to the spatial resolution of calibrated ERA5 data. The bilinear interpolation technique was selected, after comparing several other methods, due to its simplicity and being computationally inexpensive (Petrou and Petrou, 2010; Wolf et al., 2014). Though other approaches might offer better accuracy while performing the geospatial interpolation, it does not matter that much in this case, as we would again need to bias-correct the CMIP5 climatic models with respect to bias-corrected ERA5 data.

The interpolated CMIP5 data were then bias corrected using calibrated ERA5 data. The daily data from CanESM2, GFDL-ESM2M, GISS-E2-H, IPSL-CM5A-MR, IPSL-CM5A-MR and NorESM1-M climate models have no leap year (i.e. all years are 365 days in length). In Figure 2, we have compared kernel density plots (Silverman, 1986; Sheather and Jones, 1991) of the Port Vila station-based data, uncorrected ERA5, calibrated ERA5, uncorrected CMIP5 and bias-corrected CMIP5 yearly rainfall data for each of the CMIP5 models. Visually, the calibration of ERA5 and the bias correction of CMIP5 models look similar to station-based rainfall data (Figure 2). For a better comparison between each of the rainfall data sets, yearly maximum rainfall was analysed. This comparison was repeated for the six other locations in Table 1, and we observed a similarity between the station data, the calibrated ERA5 data and the bias corrected CMIP5 rainfall data sets.

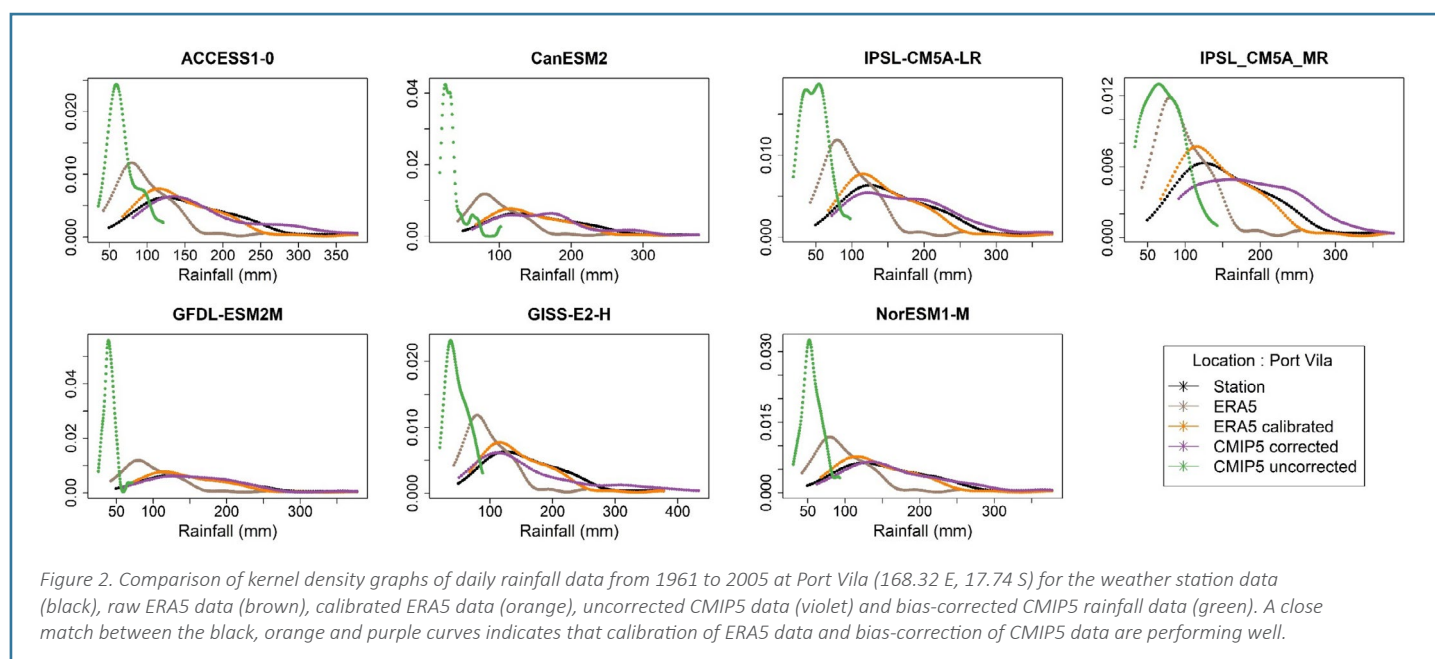




Figure 3. Climatological average daily rainfall for historical (1961–2005), RCP4.5 (2006–2100) and RCP8.5 (2006–2100) simulations from bias-corrected CMIP5 models.

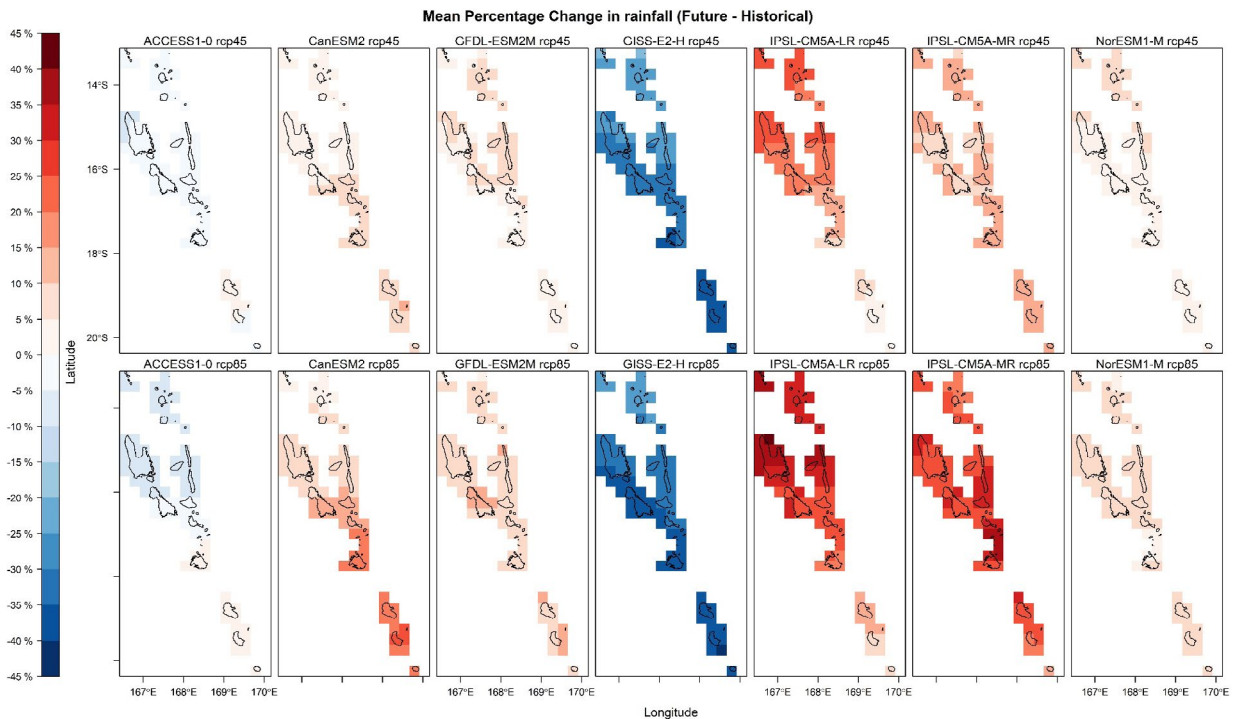


Figure 4. Mean percentage change in daily rainfall between historical (1961–2005) and future (2006–2100) simulations from bias-corrected CMIP5 models.

To examine the bias-corrected historical RCP4.5 and RCP8.5 CMIP5 rainfall data set, we have verified and validated the climatological means for 1961–2005, 2006–2100 RCP4.5 and 2006–2100 RCP8.5, respectively, over Vanuatu (Figure 3). Percentage changes in daily rainfall between historical and future scenarios have also been calculated (Figure 4). Mean daily rainfall decreases in 5 of the 7 models. As the bias corrected CMIP5 model data set was based on the calibrated ERA5 data set, the patterns persisted in the CMIP5 rainfall data set as well.

Extreme value analysis of rainfall

For extreme value analysis, we selected the two locations, Luganville, Espiritu Santo (167.22 E, 15.52 S) and Port Vila, Efate (168.32 E, 17.74 S), as examples. First, the daily bias corrected CMIP5 rainfall values were extracted for these two locations (see Figure 5) and then the annual maximum daily rainfall was computed.

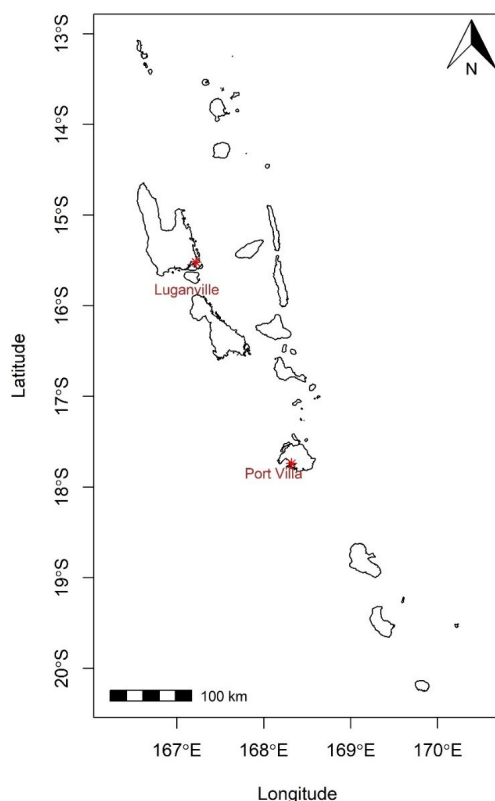


Figure 5. Map of Vanuatu showing the two locations, Luganville (167.22 E, 15.52 S) and Port Vila (168.32 E, 17.74 S).

We then computed the average recurrence interval (ARI) for various return periods. Three different periods (see Table 4) were used to compute the ARI values for 10-, 50- and 100-year return periods.

Table 4. Baseline periods for various CMIP5 climate simulations

| Baseline Period | Historical | RCP8.5 | RCP4.5 |
|-----------------|------------|--------|--------|
| 1970–2000 | X | | |
| 2040–2070 | | X | X |
| 2070–2100 | | X | X |

The Gumbel distribution was used for fitting the ARI curves (Figures 6 and 7). A previous study found the Gumbel distribution to be a very good fit for ARI curves (Mudashiru et al., 2023). Results are shown for each of the seven CMIP5 models, as well as the multi-model average (Doblas-Reyes et al., 2003; Donat et al., 2010).

The multi-model results for Port Vila and Luganville indicate a general increase in extreme rainfall intensity for a given return period, with larger increases for RCP8.5 than RCP4.5, and larger increases for 2070–2100 than 2040–2070. There is some variability between the individual climate model projections for extreme rainfall, so the projections should be treated with caution. For all return periods, the multi-model mean results for Port Vila show an increase of about 21 % for 2040–2070 RCP4.5, 30 % for 2070–2100 RCP4.5, 40 % for 2040–2070 RCP8.5 and 70 % for 2070–2100 RCP8.5. For all return periods, the multi-model mean results for Luganville show an increase of about 18 % for 2040–2070 RCP4.5, 27 % for 2070–2100 RCP4.5, 26 % for 2040–2070 RCP8.5 and 57 % for 2070–2100 RCP8.5. Appendix A includes a summary of multi-model mean results for six provinces between the historical climate (1970–2000) and the future climate (2070–2100) for RCP8.5.

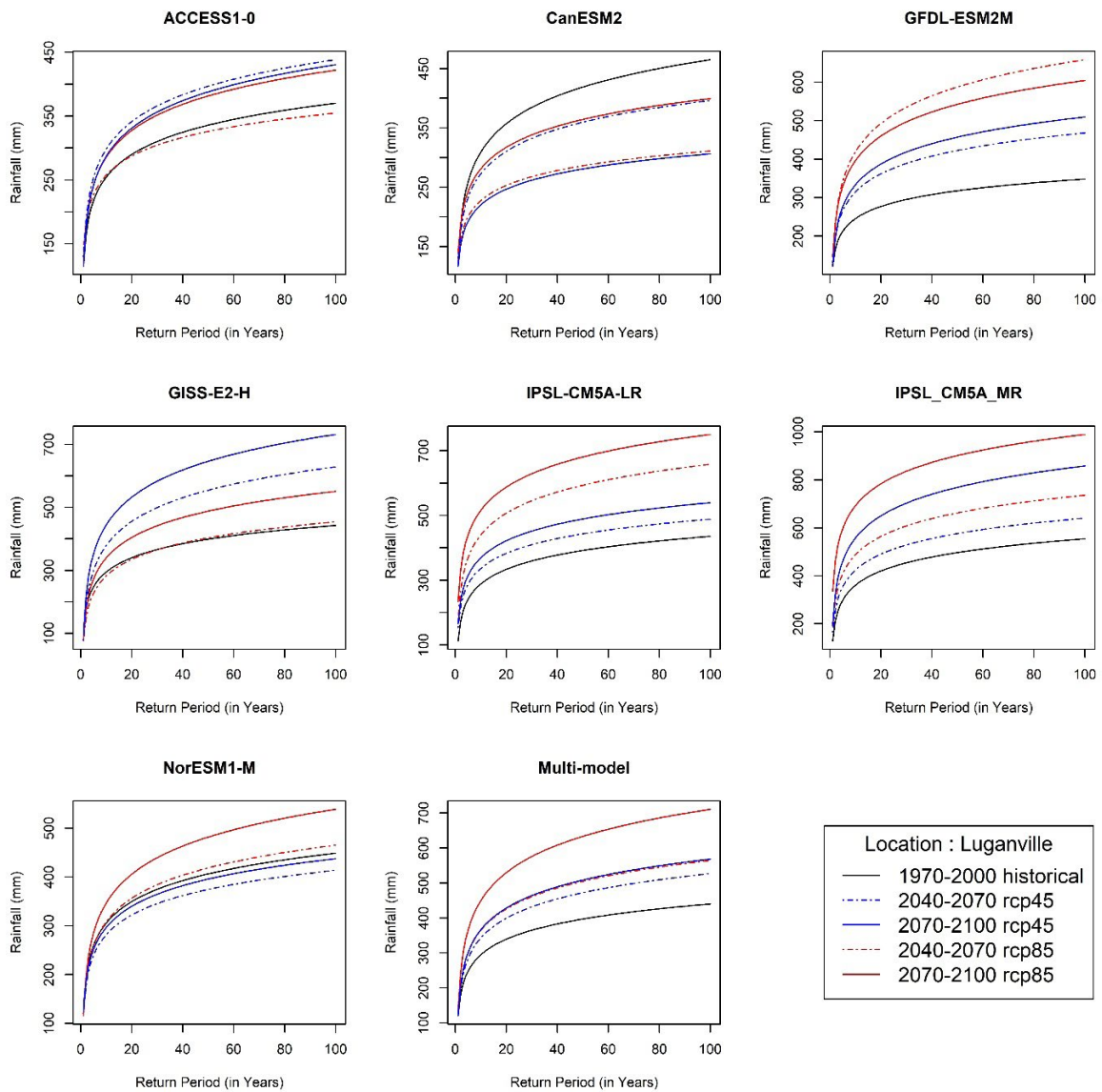


Figure 6. Average recurrence interval (ARI) curves of yearly maximum rainfall for Luganville (167.22 E, 15.52 S) using the Gumbel extreme value distribution. Comparison with historical 1970–2000 (black), RCP4.5 2040–2070 (blue dashed) RCP4.5 2070–2100 (blue), RCP8.5 2040–2070 (red dashed) and RCP8.5 2070–2100 (red) has been shown for seven climate models and the multi-model average. The multi-model mean indicates an increase in extreme rainfall intensity for a given return period.

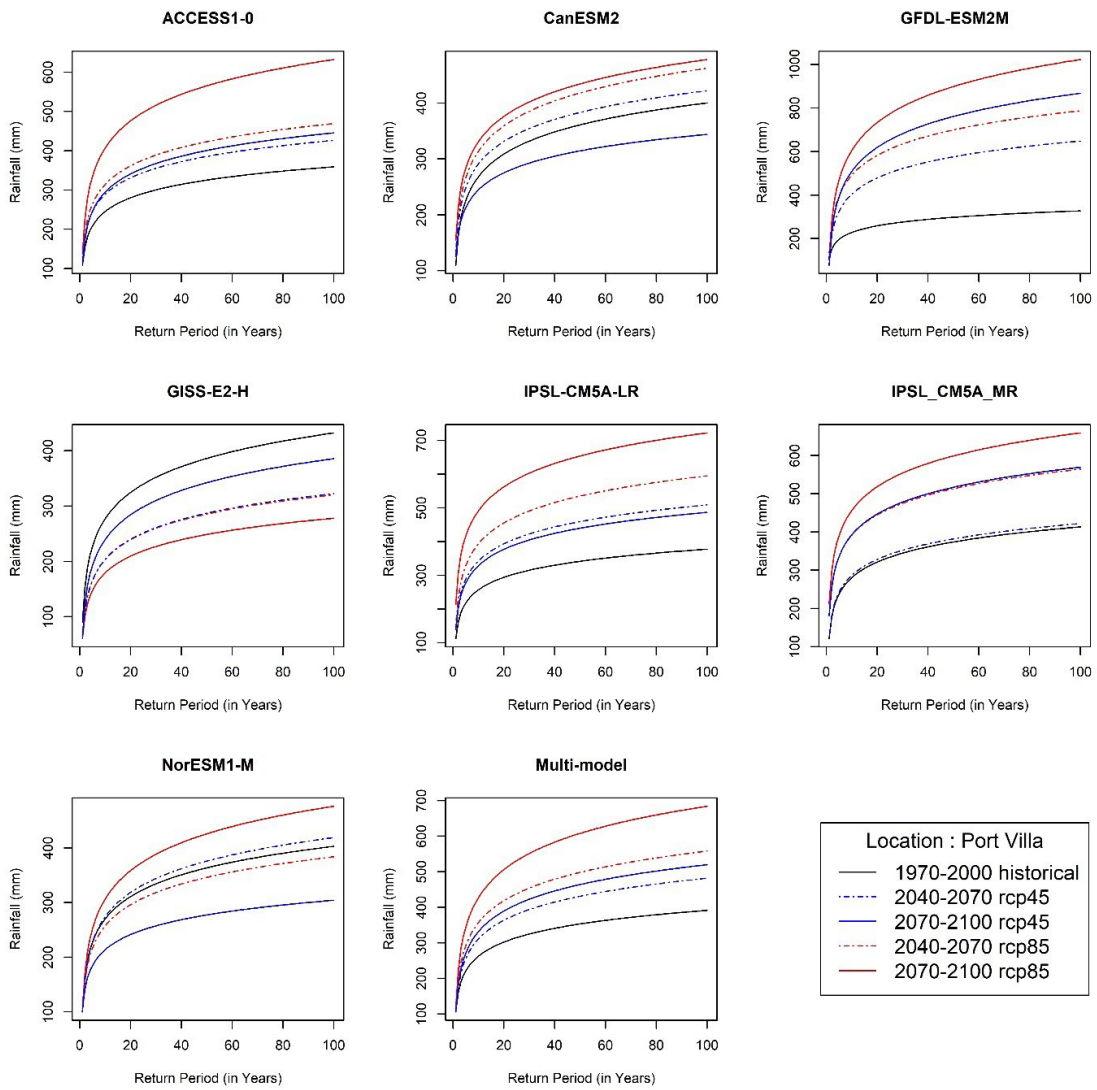


Figure 7. Average recurrence interval (ARI) curves of yearly maximum rainfall for Port Vila (168.32 E, 17.74 S) using the Gumbel extreme value distribution. Comparison with historical 1970–2000 (black), RCP4.5 2040–2070 (blue dashed) RCP4.5 2070–2100 (blue), RCP8.5 2040–2070 (red dashed) and RCP8.5 2070–2100 (red) has been shown for seven climate models and the multi-model average. The multi-model mean indicates an increase in extreme rainfall intensity for a given return period.

2. Tropical cyclone wind speed

Tropical cyclone data

The observational tropical cyclone (TC) data were sourced from the South Pacific Enhanced Archive of Tropical Cyclones database (SPEARTC) (Diamond et al., 2012), where the best track data are mostly available at 6-hour intervals for the entire TC lifecycle. The maximum 10-minute sustained wind speed in knots (Diamond et al., 2012) was converted to m/s using the conversion 1 knot = 0.51 m/s. Cyclones were also categorised according to the conventional definition of the Southern Hemisphere TC season, i.e. from 1st July to 30th June of the following year, with the following year representing a particular TC season, e.g. 1 July 2022 to 30 June 2023 is defined as the 2023 TC season.

The modelled TC data were obtained from Chand et al. (2017) and Bell et al. (2019), where they used a suite of climate models from the CMIP5 data set (Taylor et al., 2012) to simulate TCs using the Okubo-Weiss-Zeta (OWZ) detection and tracking scheme (Tory et al., 2013a; Tory et al., 2013b). Both studies evaluated two scenarios: (1) the historical-climate simulation (1970–2000) and (2) the future-climate simulation (2070–2100) under a high emissions pathway (RCP8.5). These data sets also included 850 hPa wind speeds that were converted to surface winds using a conversion factor of 0.8 (Franklin et al., 2003). We evaluated simulated TC tracks from 13 models (Table 5) for both historical and future scenarios.

Table 5. List of 13 CMIP5 models used for TC wind speed analysis along with time periods for the historical and future (RCP8.5) scenarios, based on data availability.

| Models | Historical period | Future period (RCP8.5) |
|--------------------|-------------------|------------------------|
| SPEARTC | 1970–2000 | |
| ACCESS1.0 | 1970–2000 | 2070–2100 |
| ACCESS1.3 | 1970–2000 | 2070–2100 |
| BCC-CSM1.1 | 1970–2000 | 2069–2099 |
| BCC-CSM1.1M | 1970–2000 | 2070–2100 |
| CCSM4 | 1970–2000 | 2070–2100 |
| CNRM-CM5 | 1970–2000 | 2070–2100 |
| CSIRO-MK3.6 | 1970–2000 | 2070–2100 |
| GFDL-CM3 | 1970–2000 | 2070–2100 |
| GFDL-ESM2G | 1970–2000 | 2070–2100 |
| GFDL-ESM2M | 1970–2000 | 2070–2100 |
| HadGEM2-ES | 1970–2000 | 2069–2099 |
| MIROC5 | 1970–2000 | 2070–2100 |
| MRI-CGCM3 | 1970–2000 | 2070–2100 |

Data mining and quality control

Three buffer regions (Figure 8) were created (50 km, 250 km and 500 km) around all of Vanuatu, followed by a 500 km buffer around each of the six provinces. These three buffers were used to extract TC tracks from all three data sets (i.e. SPEArTC, 13 historical simulations and 13 RCP8.5 simulations) for the whole Vanuatu region, as well as for each province using the 500 km buffer. The data were then quality checked, ensuring that all TC track points (6-hour timestep for SPEArTC and 12-hour for CMIP5 models) within each buffer were extracted. For cases where a TC track traversed the buffer region but without a 6-hour (for SPEArTC) or 12-hour (for climate models) timestep, a timestep was estimated (especially for the 850 hPa TC wind speed) via a simple interpolation.

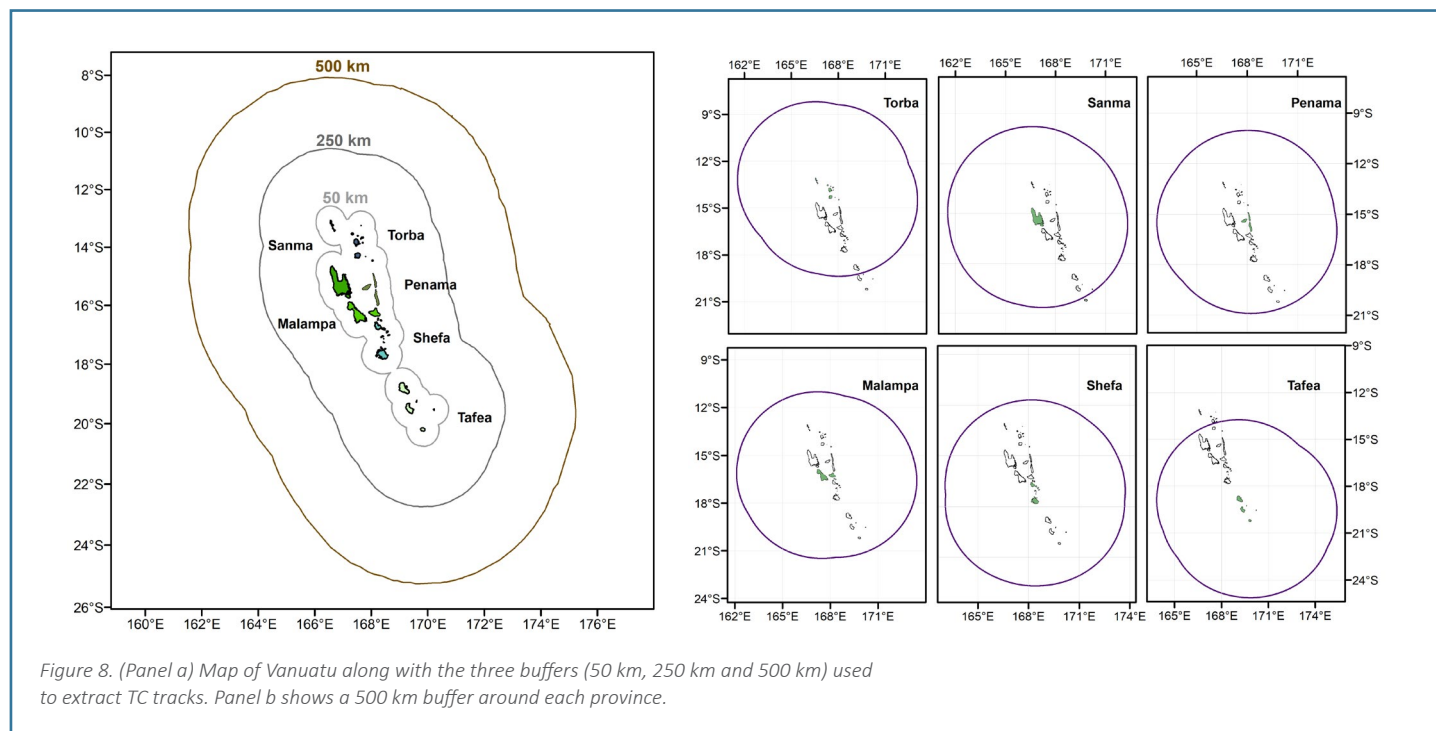


Figure 8. (Panel a) Map of Vanuatu along with the three buffers (50 km, 250 km and 500 km) used to extract TC tracks. Panel b shows a 500 km buffer around each province.

Statistical calibration

The TC wind speeds extracted from the climate models were calibrated so that the reconstructed data resembled the observed data as closely as possible. This was achieved using quantile matching with the help of a cubic spline approach, as discussed above. The 13 CMIP5 climate models (Table 6) for historical and RCP8.5 scenarios were calibrated with respect to the observational data (SPEArTC) (Figure 9). A bin size of 10 was determined using the Root Mean Square Estimate (RMSE) (Biswas et al., 2022).

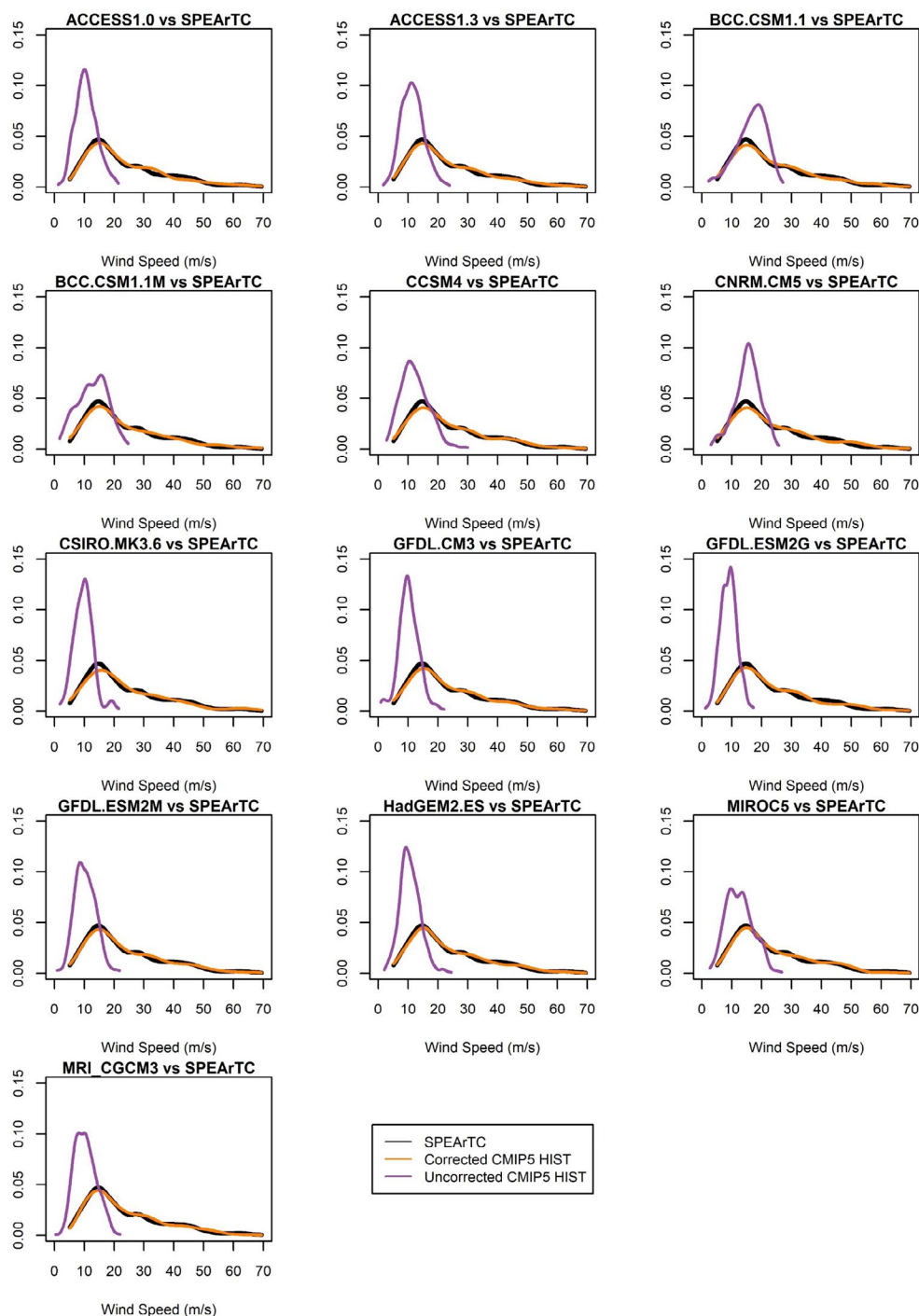


Figure 9. Kernel density graphs of TC wind speed data for 1970–2000 (within the 500 km buffer) using the cubic spline method. Each graph illustrates the observed data (SPEArTC in black), uncorrected CMIP5 data (purple) and bias-corrected model data (orange). A close match between the SPEArTC data and corrected CMIP5 data indicates that the calibration method is performing well.

Temporal analyses

The calibrations applied to the historical climate model data were also applied to the future climate model data. This bias-corrected data set was then used to collate TC intensity information for each province, followed by a quality check, as mentioned above. TCs with wind speed reaching 17.5 m/s during 1970–2000 (representing the late 20th century) and 2070–2100 (late 21st century) were considered for further analyses. For two models, BCC-CSM1.1 and HadGEM2-ES, their late 21st century period is 2069–2099 (see Table 5).

An additional step was taken to identify the best-performing models because Bell et al. (2019) highlighted some caveats associated with the outputs from the OWZ TC detector. Their study showed that the TC detection scheme sometimes tends to underestimate or overestimate TC frequency, potentially impacting the projection assessments. Bell et al. (2019) objectively defined specific measures to eliminate errors and achieve a more accurate climatology. We used one such definition: the number of simulated TCs should be within $\pm 50\%$ of the TC counts in SPEArTC (i.e. the observed climatology). Using this criterion, the eight best-performing models were selected for all analyses in this study (Table 6). These eight models were also identified as the best-performing models by Chand et al. (2017).

Table 6. Total number of TCs extracted within each buffer for all 13 CMIP5 models (both historical and RCP8.5). The bold TC numbers indicate the best-performing models that simulated at least 50% of total observed TCs from SPEArTC (red).

| Climate models | Historical TCs | | | RCP8.5 TCs | | |
|--------------------|----------------|------------|------------|------------|--------|-------|
| | 500 km | 250 km | 50 km | 500 km | 250 km | 50 km |
| SPEArTC | 105 | 73 | 40 | | | |
| ACCESS1.0 | 69 | 51 | 27 | 73 | 49 | 27 |
| ACCESS1.3 | 82 | 57 | 33 | 124 | 90 | 46 |
| BCC-CSM1.1 | 51* | 24* | 14* | 42 | 24 | 12 |
| BCC-CSM1.1M | 41 | 24 | 8 | 49 | 26 | 9 |
| CCSM4 | 41 | 35 | 19 | 32 | 22 | 13 |
| CNRM-CM5 | 27 | 18 | 10 | 17 | 10 | 4 |
| CSIRO-MK3.6 | 32 | 19 | 11 | 73 | 48 | 33 |
| GFDL-CM3 | 42 | 30 | 20 | 31 | 17 | 4 |
| GFDL-ESM2G | 57 | 34* | 10* | 41 | 24 | 10 |
| GFDL-ESM2M | 59 | 36* | 17* | 44 | 23 | 9 |
| HadGEM2-ES | 80 | 53 | 32 | 55 | 31 | 14 |
| MIROC5 | 89 | 52 | 29 | 53 | 33 | 16 |
| MRI-CGCM3 | 109 | 65 | 42 | 91 | 63 | 41 |

* Even though this model's climatology is not within $\pm 50\%$ of SPEArTC, either/or it is very close, and has been identified as a best performing model by Chand et al. (2017); hence, it was included for further analyses.

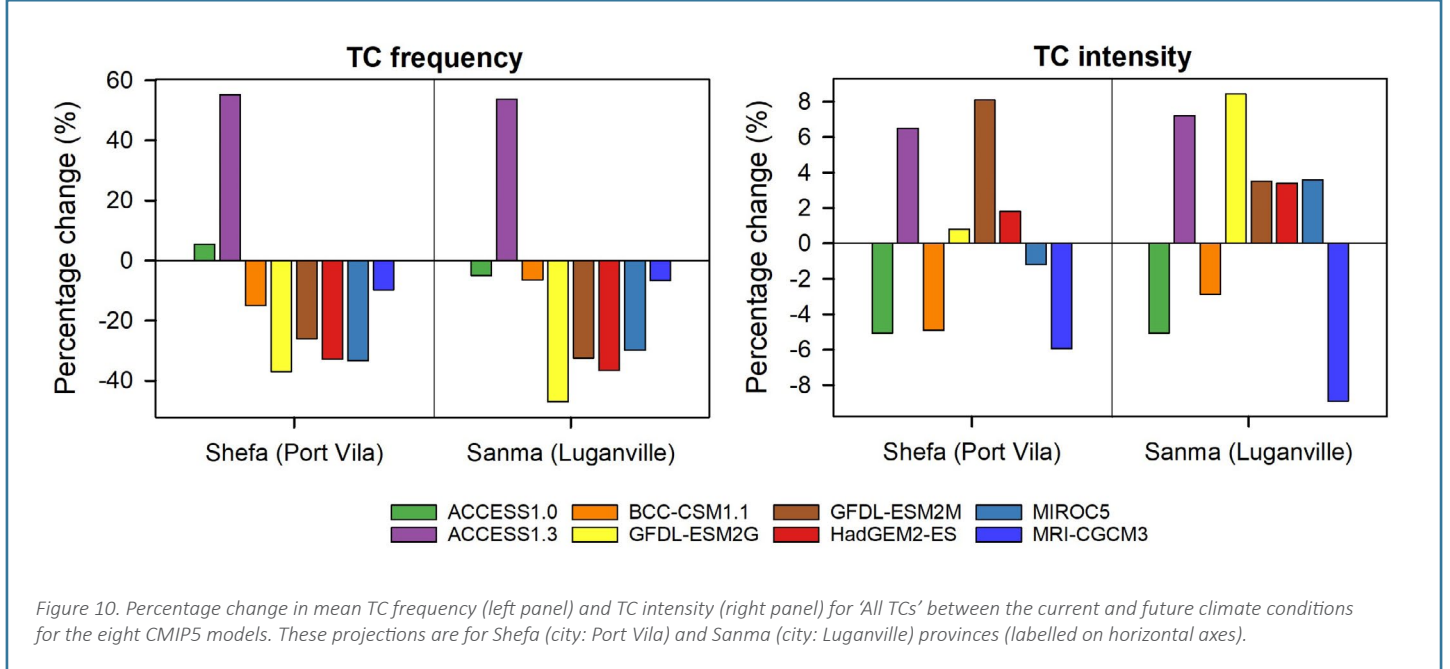
For all analyses, we used the maximum TC wind speed along the TC track within the buffer as our emphasis is on extremes. We evaluated the TC climatology as per the observational data (timeseries for the 1971–2021 TC season) at the national and provincial levels. Projected changes in TC intensity and frequency from the selected models were assessed in two ways (both at national and provincial levels): firstly, by evaluating 'All TCs' (from categories 1 to 5) and secondly, only considering 'Severe TCs' (categories 3 to 5) (also see Appendix B). TCs were sorted into respective categories using the Australian TC intensity scale (Table 7). In both cases, TC intensities and TC frequencies were contrasted between the current and future climate conditions. Consequently, projected changes in these TC metrics (frequency and intensity) were derived by computing their percentage changes. The Gumbel function was used to construct ARIs. We also combined the eight models to form a multi-model average and performed similar analyses.

Table 7. TC classification is based on the Australia/Fiji intensity scale. Maximum wind refers to the 10-minute sustained wind speed.

| Category | Maximum wind (km/hr) |
|----------|----------------------|
| 1 | 63–88 |
| 2 | 89–117 |
| 3 | 118–159 |
| 4 | 160–200 |
| 5 | > 200 |

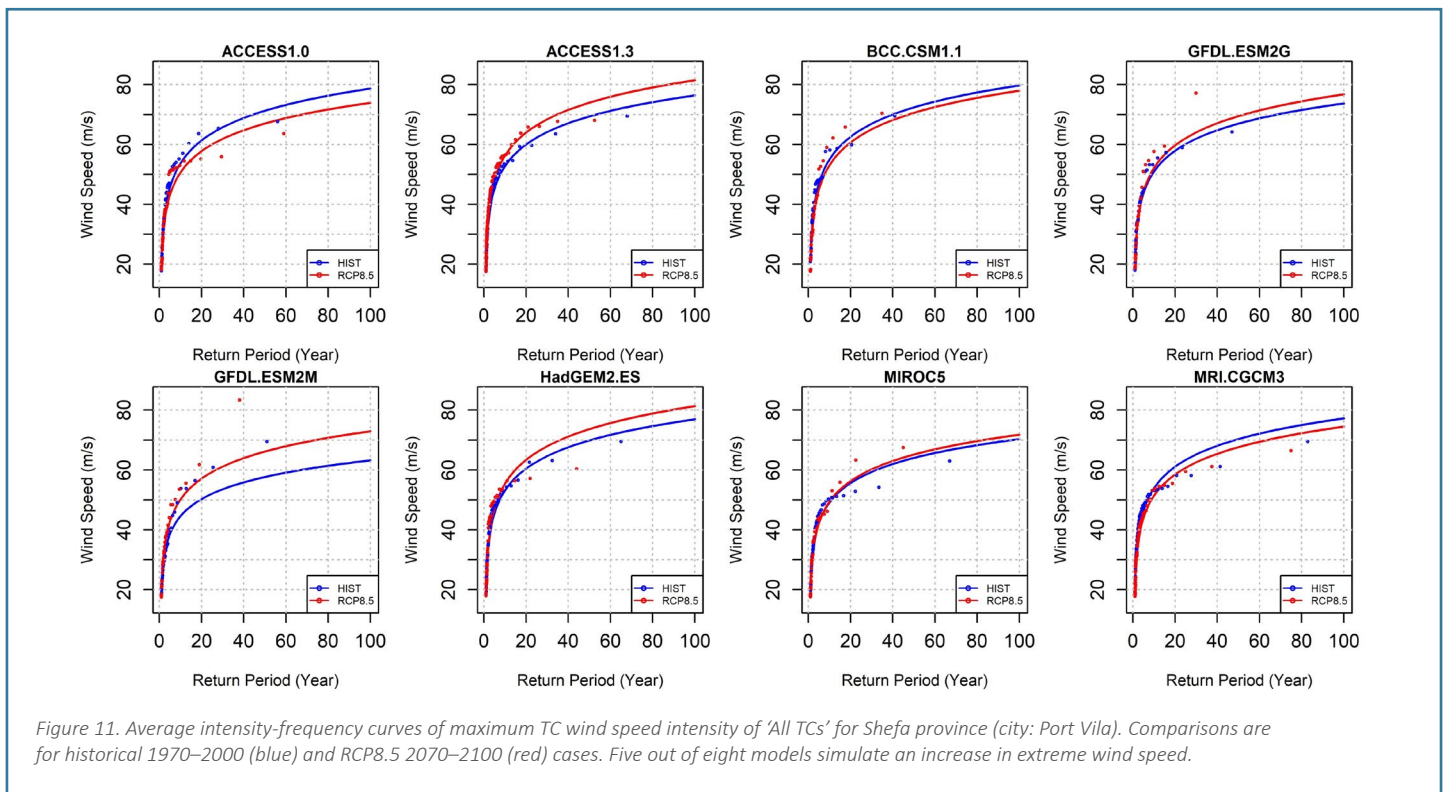
Projected changes in TC frequency and intensity

The projected changes in TC frequency and TC intensity for 'All TCs' are shown in Figure 10 for the two provinces: Shefa (including the city of Port Vila) and Sanma (including the city of Luganville). Out of eight models, six and seven models demonstrate a projected decrease in TC frequency in future for Shefa and Sanma provinces, respectively (Figure 10, left panel). Conversely, TC intensities are projected to increase at both locations, indicated by four (for Shefa) and five (for Sanma) models (Figure 10, right panel).



Intensity-frequency curves for All TCs

TC intensity-frequency changes between historical and future periods are shown below for two provinces: Shefa (which includes Port Vila; Figure 11) and Sanma (which includes Luganville; Figure 12). Most models simulate an increase in extreme wind speeds. The multi-model mean for Shefa indicates that the increase is about 3% for all return periods (Figure 13, top row). The multi-model mean for Sanma indicates that the increase is about 3% for all return periods (Figure 13, bottom row). Appendix B includes a summary of multi-model mean changes for all six provinces, which range from 2–5%.



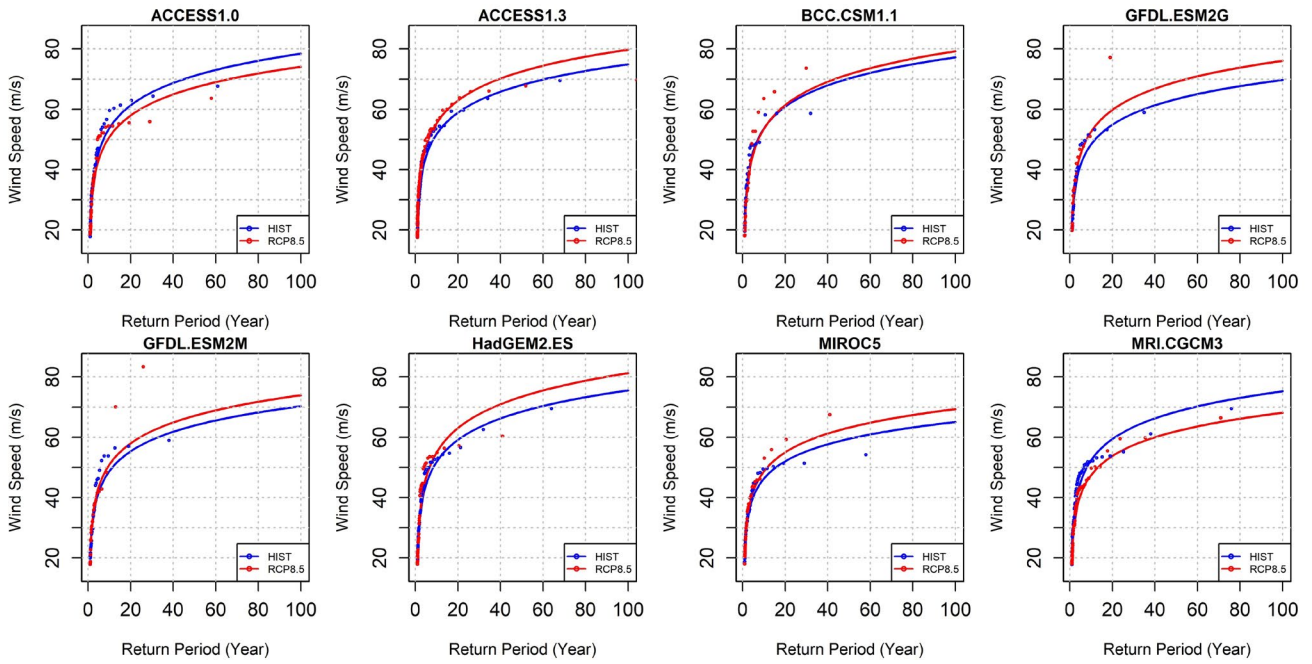
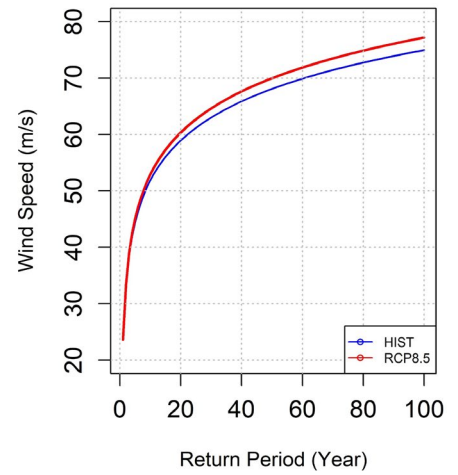
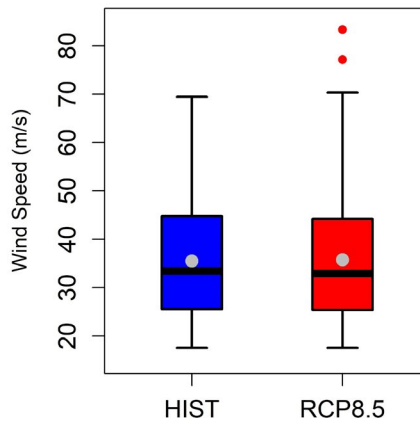


Figure 12. As in Figure 11, but for Sanma Province (city: Luganville). Six out of eight models simulate an increase in extreme wind speed.

**Shefa
(Port Vila)**



**Sanma
(Luganville)**

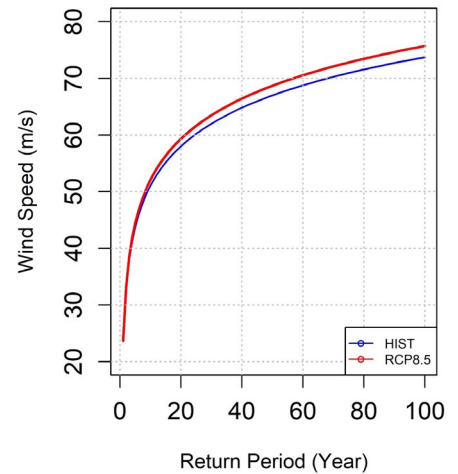
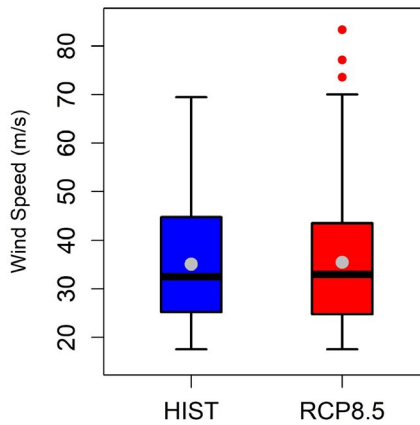


Figure 13. TC wind speed distribution (left) and ARIs (right) of all eight models combined to form a multi-model average of 'All TCs' for Shefa (city: Port Vila; top row) and Sanma (city: Luganville; bottom row) provinces. The multi-model average at both locations shows a small increase in extreme wind speed.

Discussion

In this study, we assessed projected changes in extreme rainfall and wind speed for Vanuatu.

We have used ARI curves to show the projected change in annual maximum daily rainfall for 2040–2070 and 2070–2100 for low and high emissions pathways. A general increase in extreme rainfall intensity is simulated for both Port Vila and Luganville. There are some differences in ARI curves between climate models. For example, GISS-E2-H shows a decrease in extreme rainfall intensities at Port Vila while CanESM2 shows a decrease at Luganville. So, the projections should be interpreted with caution. The extreme rainfall data can be used in current and future flood risk assessments. New Zealand's NIWA is undertaking an ADB-sponsored flood risk assessment for Luganville that incorporates our extreme rainfall projections and overlays an exposure database that includes buildings and infrastructure. This will inform adaptation planning.

We also used ARI curves to assess projected changes in TC frequency and intensity. Assessing the vulnerability of a specific region to TCs is an essential step in formulating enhanced strategies for disaster preparedness. Overall, the projections indicated a decline in TC frequencies and mixed changes in TC intensities – consistent with previous findings (Tory *et al.*, 2013; Walsh *et al.*, 2016; Chand *et al.*, 2017; Bell *et al.*, 2019; Knutson *et al.*, 2020; CSIRO and SPREP, 2021). Projections derived from the other two buffers (i.e. 250 km and 50 km) revealed consistent trends, adding more lines of evidence to support our findings. It is worth mentioning that the consensus found in these other studies was generally for the broader South Pacific area. However, our findings offer additional evidence concerning the projections of both frequency and intensity of TCs for Vanuatu.

The results from provincial analyses were insightful, given that they demonstrated the hazards different regions are likely to encounter due to TCs when approaching the end of the 21st century. For instance, the 5 % increase in intensity derived for Torba province (in the north) is larger than the 2 % increase at Tafea (in the north).

The information gained from these projections is important for adaptation and planning. Port Vila and Luganville are the most populous areas with the largest number of buildings and infrastructure, and therefore are at risk from the greatest potential loss and damage from TCs, including critical infrastructure, disruption of livelihoods, threats to water and food security, compromising health and affecting education. One study estimated that 5145 buildings in Luganville and 2115 buildings in Port Vila are at risk of heavy damage from an extreme wind event with a 100-year return period (Beca, GNS and NIWA, 2016). UN.ESCAP (2021) has indicated that Vanuatu's expenses (approx. USD 1.1 billion) sustained from natural disasters could increase to USD 1.4 billion in a worst case scenario (RCP8.5), which can risk the country losing about 20 % of its annual gross domestic product. Hence, relevant agencies (e.g. Meteorological Services, National Disaster Management Offices and Departments of Climate Change) could utilise extreme rainfall and wind speed information to enhance awareness, risk assessment and adaptation processes. It is also crucial that this information is clearly communicated to sector stakeholders and the wider community through their information products and awareness programmes.

Conclusions

Extreme daily rainfall intensity is expected to increase in the future due to climate change. Historical weather station data, reanalysis data, seven climate model simulations and extreme value analysis were combined to estimate current and future extreme rainfall for Vanuatu. The current baseline was defined as 1970–2000, while the future periods were 2040–2070 and 2070–2100. Low (RCP4.5) and high (RCP8.5) greenhouse gas emissions scenarios were considered. For extreme daily rainfall with return periods of 10–100 years, the multi-model mean results for Port Vila showed an increase of about 21 % for 2040–2070 RCP4.5, 30 % for 2070–2100 RCP4.5, 40 % for 2040–2070 RCP8.5 and 70 % for 2070–2100 RCP8.5. For return periods of 10–100 years, the multi-model mean results for Luganville showed an increase of about 18 % for 2040–2070 RCP4.5, 27 % for 2070–2100 RCP4.5, 26 % for 2040–2070 RCP8.5 and 57 % for 2070–2100 RCP8.5. Similar increases were found for all six Vanuatu provinces. These increases have significant implications for future flood risk management strategies.

Although Vanuatu is experienced in responding to cyclones, a double event such as TC Judy and TC Kevin in March 2023 presented unprecedented challenges. Tropical cyclones are projected to become less frequent, but the average intensity is projected to increase. Therefore, developing a more comprehensive understanding of cyclone behaviour is essential to inform adaptation strategies across different sectors. Such understanding can also enhance the general public's resilience to the destructive impacts of extreme events, particularly in a worst-case scenario. Reanalysis data, eight climate model simulations and extreme value analysis were combined to estimate current and future extreme wind speeds for Vanuatu. The current baseline was defined as 1970–2000, while the future period was 2070–2100. A high (RCP8.5) greenhouse gas emissions scenario was considered. For extreme TC wind speeds with return periods of 10–100 years, the multi-model mean results showed an increase in the intensity of about 3 % for Port Vila and Luganville. Increases of 2–5 % were found for all six Vanuatu provinces. These small increases may have implications for future cyclone risk management strategies.

Additionally, decision-makers such as environmental managers and city planners can use these projections along with suitable exposure and vulnerability data to undertake detailed risk assessments in Vanuatu. This can facilitate more effective adaptation strategies across various sectors, complementing previous findings (e.g. Beca, GNS and NIWA, 2016).

References

1. Beca, GNS and NIWA (2016). Urban Risk Assessment and Geo-data Management Report: Risk Mapping and Planning for Urban Preparedness (Contract No. C.06). Prepared for Vanuatu Meteorological and Geo-hazards Department by Beca International Consultants Ltd (Beca), GNS Science and the National Institute of Water and Atmospheric Research (NIWA), 228 pages.
2. Bell SS, Chand SS, Camargo SJ, Tory KJ, Turville C, Ye H (2019) Western North Pacific Tropical Cyclone Tracks in CMIP5 Models: Statistical Assessment Using a Model-Independent Detection and Tracking Scheme. *Journal of Climate* 32:7191-7208. <https://doi.org/https://doi.org/10.1175/JCLI-D-18-0785.1>
3. Biswas S, Chand SS, Dowdy AJ, Wright W, Foale C, Zhao X, Deo A (2022) Statistical Calibration of Long-Term Reanalysis Data for Australian Fire Weather Conditions. *Journal of Applied Meteorology and Climatology* 61:729-758. <https://doi.org/10.1175/jamc-d-21-0034.1>
4. Chand SS, Tory KJ, Ye H, Walsh KJE (2017) Projected increase in El Niño-driven tropical cyclone frequency in the Pacific. *Nature Climate Change* 7:123-127. <https://doi.org/10.1038/nclimate3181>
5. CSIRO and SPREP. (2022). *Tropical Cyclones and Climate Change: implications for the Western Tropical Pacific*. <https://doi.org/https://doi.org/10.25919/pbtc-1y82>
6. CSIRO and SPREP. (2021). "NextGen" Projections for the Western Tropical Pacific: Current and Future Climate for Vanuatu. <https://doi.org/https://doi.org/10.25919/hexz-1r10>
7. Diamond HJ, Lorrey AM, Knapp KR, Levinson DH (2012) Development of an enhanced tropical cyclone tracks database for the southwest Pacific from 1840 to 2010. *International Journal of Climatology* 32:2240-2250. <https://doi.org/https://doi.org/10.1002/joc.2412>
8. Doblus-Reyes FJ, Pavan V, Stephenson DB (2003) The skill of multi-model seasonal forecasts of the wintertime North Atlantic Oscillation. *Climate Dynamics* 21:501-514. <https://doi.org/10.1007/s00382-003-0350-4>
9. Donat MG, Leckebusch GC, Wild S, Ulbrich U (2010) Benefits and limitations of regional multi-model ensembles for storm loss estimations. *Climate Research* 44:211-225. <https://www.int-res.com/abstracts/cr/v44/n2-3/p211-225/>
10. Franklin JL, Black ML, Valde K (2003) GPS Dropwindsonde Wind Profiles in Hurricanes and Their Operational Implications. *Weather and Forecasting* 18:32-44. [https://doi.org/https://doi.org/10.1175/1520-0434\(2003\)018<0032:GDWPIH>2.0.CO;2](https://doi.org/https://doi.org/10.1175/1520-0434(2003)018<0032:GDWPIH>2.0.CO;2)
11. Knutson T, Camargo SJ, Chan JCL, Emanuel K, Ho CH, Kossin J, Mohapatra M, Satoh M, Sugi M, Walsh K, & Wu L, (2020). Tropical cyclones and climate change assessment. *Bulletin of the American Meteorological Society*, 100(10), 1987–2007. <https://doi.org/10.1175/BAMS-D-18-0189.1>
12. Li J, Heap AD (2014) Spatial interpolation methods applied in the environmental sciences: A review. *Environmental Modelling & Software* 53:173-189. <https://doi.org/10.1016/j.envsoft.2013.12.008>
13. Moss RH, Edmonds JA, Hibbard KA, Manning MR, Rose SK, van Vuuren DP, Carter TR, Emori S, Kainuma M, Kram T, Meehl GA, Mitchell JFB, Nakicenovic N, Riahi K, Smith SJ, Stouffer RJ, Thomson AM, Weyant JP, Wilbanks TJ (2010) The next generation of scenarios for climate change research and assessment. *Nature* 463:747-756. <https://doi.org/10.1038/nature08823>
14. Mudashiru RB, Abustan I, Sabtu N, Mukhtar HB, Balogun W (2023) Choosing the best fit probability distribution in rainfall design analysis for Pulau Pinang, Malaysia. *Modeling Earth Systems and Environment*. <https://doi.org/10.1007/s40808-022-01668-0>
15. Petrou M, Petrou C (2010) Image Restoration. *Image Processing: The Fundamentals*. pp 395-526.
16. Piani C, Weedon GP, Best MJ, Gomes SM, Viterbo PA, Hagemann S, Haerter JO (2010) Statistical bias correction of global simulated daily precipitation and temperature for the application of hydrological models. *Journal of Hydrology* 395:199-215. <https://doi.org/10.1016/j.jhydrol.2010.10.024>
17. Sheather SJ, Jones MC (1991) A Reliable Data-Based Bandwidth Selection Method for Kernel Density Estimation. *Journal of the Royal Statistical Society Series B (Methodological)* 53:683-690. <http://www.jstor.org/stable/2345597>
18. Silverman B (1986) *Density Estimation for Statistics and Data Analysis*. Chapman and Hall, London.
19. Taylor KE, Stouffer RJ, Meehl GA (2012) An Overview of CMIP5 and the Experiment Design. *Bulletin of the American Meteorological Society* 93:485-498. <https://doi.org/10.1175/bams-d-11-00094.1>
20. Teutschbein C, Seibert J (2012) Bias correction of regional climate model simulations for hydrological climate-change impact studies: Review and evaluation of different methods. *Journal of Hydrology* 456-457:12-29. <https://doi.org/10.1016/j.jhydrol.2012.05.052>
21. Tory KJ, Chand SS, Dare RA, McBride JL (2013a) The Development and Assessment of a Model-, Grid, and Basin-Independent Tropical Cyclone Detection Scheme. *Journal of Climate* 26:5493-5507. <https://doi.org/https://doi.org/10.1175/JCLI-D-12-00510.1>
22. Tory KJ, Dare RA, Davidson NE, McBride JL, Chand SS (2013b) The importance of low-deformation vorticity in tropical cyclone formation. *Atmos Chem Phys* 13:2115-2132. <https://doi.org/10.5194/acp-13-2115-2013>
23. Tory KJ, Chand SS, McBride JL, Ye H, & Dare RA, (2013). Projected Changes in Late-Twenty-First-Century Tropical Cyclone Frequency in 13 Coupled Climate Models from Phase 5 of the Coupled Model Intercomparison Project. *Journal of Climate*, 26(24), 9946–9959. <https://doi.org/10.1175/JCLI-D-13-00010.1>
24. UN.ESCAP. (2021). Resilience in a riskier world: managing systemic risks from biological and other natural hazards. In *Asia Pacific Disaster Report 2021*. <https://hdl.handle.net/20.500.12870/3811>
25. van Vuuren DP, Edmonds J, Kainuma M, Riahi K, Thomson A, Hibbard K, Hurtt GC, Kram T, Krey V, Lamarque J-F, Masui T, Meinshausen M, Nakicenovic N, Smith SJ, Rose SK (2011) The representative concentration pathways: an overview. *Climatic Change* 109:5. <https://doi.org/10.1007/s10584-011-0148-z>
26. Walsh KJEE, McBride JL, Klotzbach PJ, Balachandran S, Camargo SJ, Holland G, Knutson TR, Kossin JP, Lee T cheung, Sobel A, & Sugi M, (2016). Tropical cyclones and climate change. *Wiley Interdisciplinary Reviews: Climate Change*, 7(1), 65–89. <https://doi.org/doi:10.1002/wcc.371>
27. Wolf PR, Dewitt BA, Wilkinson BE (2014) *Digital Resampling*. Fourth edition. edn. McGraw-Hill Education, New York

Appendix A: Summary of projected changes in extreme rainfall across provinces under a high emissions pathway

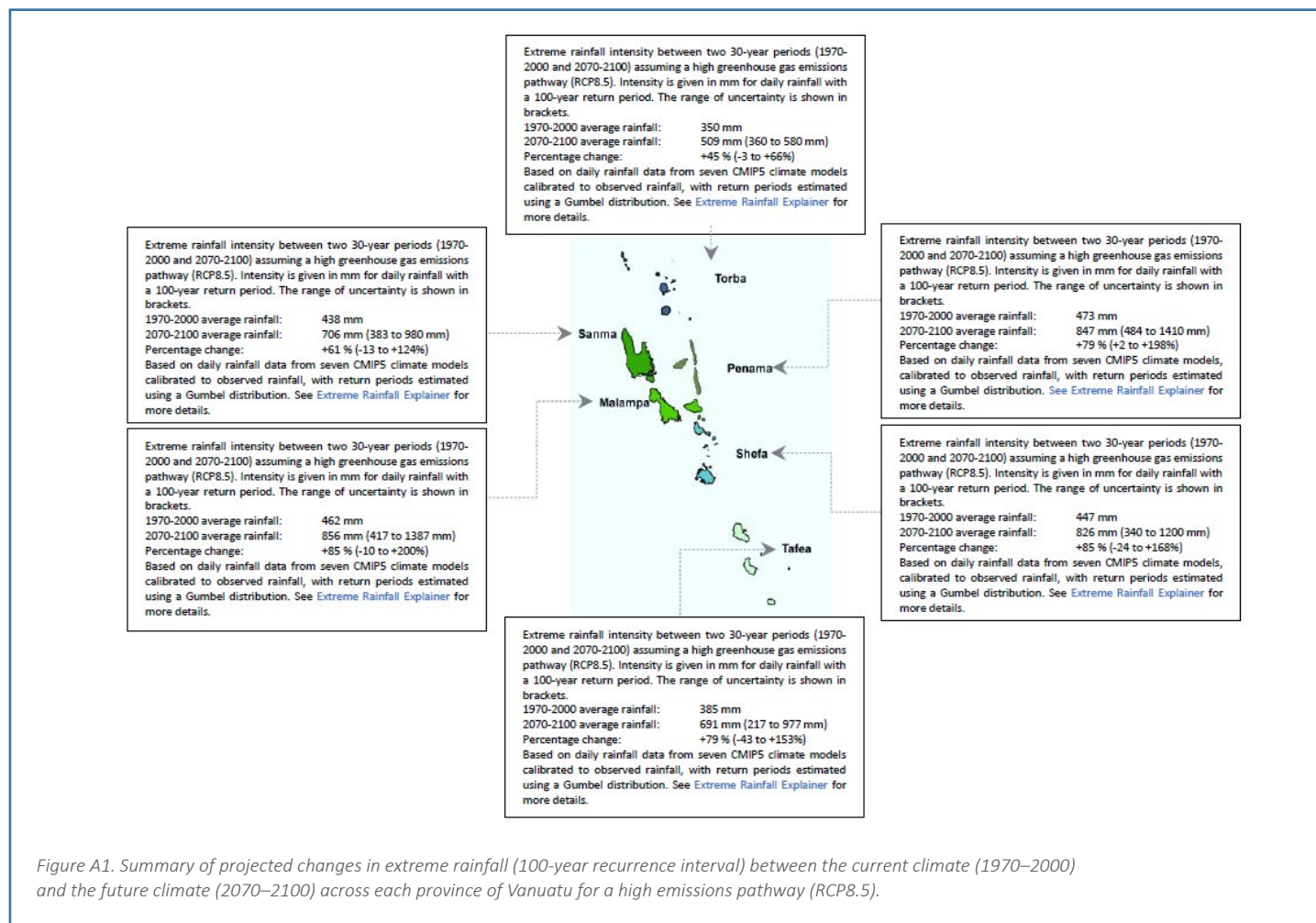


Figure A1. Summary of projected changes in extreme rainfall (100-year recurrence interval) between the current climate (1970–2000) and the future climate (2070–2100) across each province of Vanuatu for a high emissions pathway (RCP8.5).

Appendix B: Summary of projected changes in cyclone wind speed intensity across provinces under a high emissions pathway

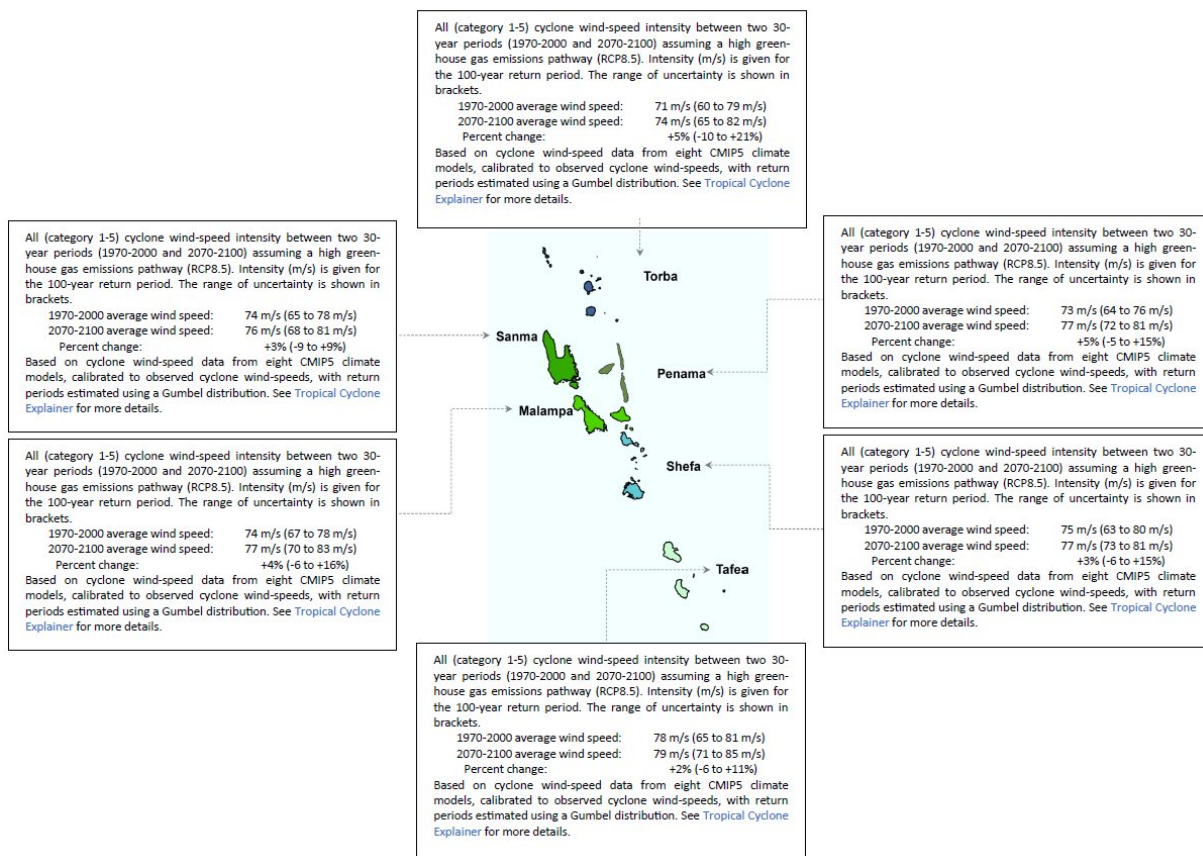


Figure B1. Summary of projected changes in cyclone wind speed intensity (categories 1–5, 100-year recurrence interval) between the current climate (1970–2000) and the future climate (2070–2100) across each province of Vanuatu for a high emissions pathway (RCP8.5).

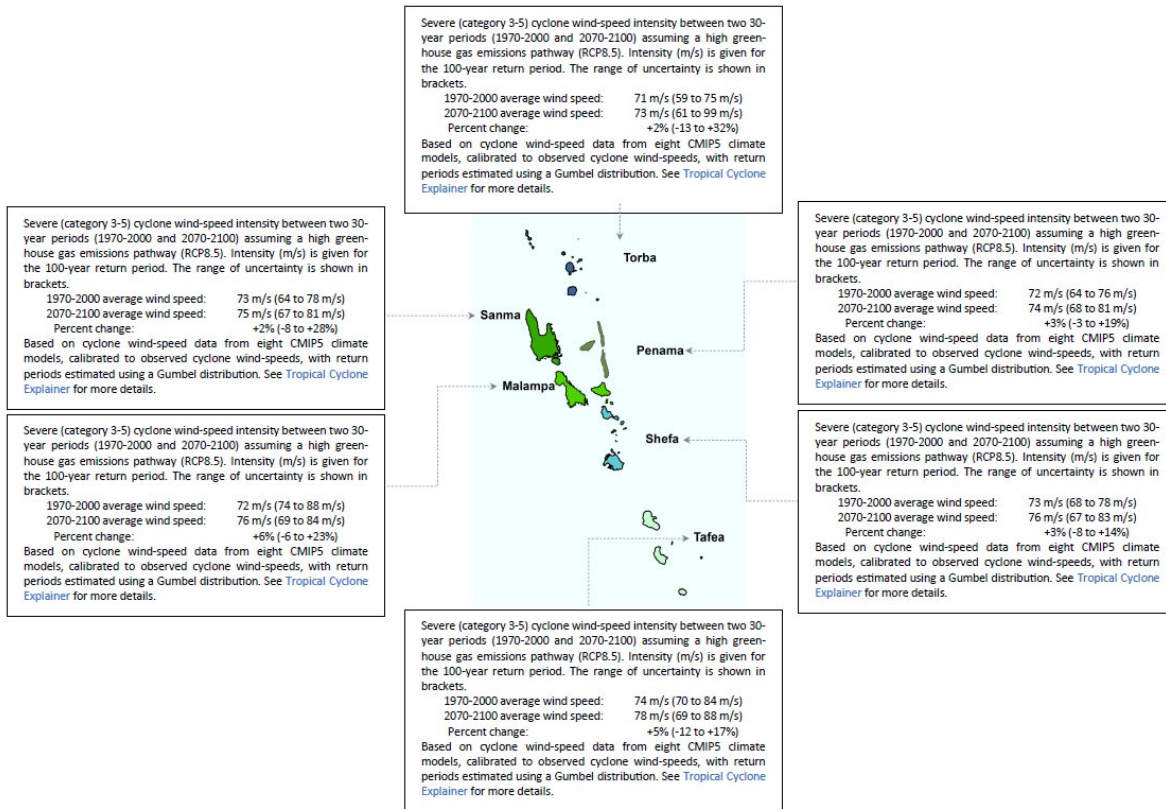


Figure B2. As in Figure B1, but for “Severe cyclones”, that is, category 3–5.